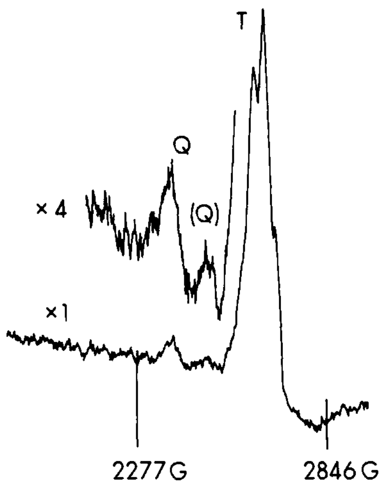

Figure 6. ESR spectrum of quintet radical pair (Q) and the H_{z1} line of triplet **1b** (T) generated in the photolysis of 3-diazohexafluoro-2-butanone polycrystal at 18 K. The klystron frequency was 9.371 GHz.

carbene, indicating that at 10 K intersystem crossing competes favorably with the Wolff rearrangement (eq 11).

$$cis\text{-}CF_3CN_2COCF_3 + h\nu \xrightarrow{-N_2} cis\text{-}CF_3CCOCF_3(S_1) \qquad (13)$$

$$cis\text{-}CF_3CCOCF_3(S_1) \xrightarrow{ICS} cis\text{-}CF_3CCOCF_3(T_0) \qquad (14)$$

The temperature dependence of signal intensities was also examined in the 8–50 K range and the results are plotted in Figure 5. The signal intensity changes are reversible and the intensity of the cis conformer clearly obeys the Curie law. The data on the trans conformer are scattered but also appear to follow the Curie law. The linearity of the plots in Figure 5 is consistent with a triplet ground state or with a near degenerate triplet–singlet state. The former is likely.

In addition to the triplet spectra discussed above, the other weak but well-reproducible transitions were observed in the 2300–2500 G range, Figure 6. These appeared in the polycrystal but not in the neat glass photolysis and only at $T \leq 40$ K. From previous studies on triplet benzoylphenylmethylene,[5] 9-oxo-10-anthrylene,[9] and pivaloyl-*tert*-butylmethylene[22] we known that the quintet state radical pairs which have been shown to form in these systems from the interaction of two close neighbor triplet carbenes exhibit weak absorptions in this spectral range corresponding to $m = 0 \rightarrow |m| = 1$ transitions. These occur at H_z, H_y, and H_x of about 2360, 2620, and 2670 G for benzoylphenylmethylene, 2300, 2490, and 2530 G for 9-oxo-10-anthrylene, and 2300 and 2450 G for pivaloyl-*tert*-butylmethylene, respectively. On the basis of the close similarity among these spectra in regard to location and intensity, nonappearance in glassy matrix photolysis, low thermal stability, and persistent good reproducibility we assign these absorptions to the quintet state radical pairs formed from two neighbor **1** molecules.

Acknowledgment. We thank the Natural Science and Engineering Research Council of Canada for financial support.

---

(22) Murai, H.; Ribo, J.; Torres, M.; Strausz, O. P., to be published.

(23) Trozzolo, A. M.; Fahrenholtz, S. R., Abstracts of papers, 151st National Meeting of the American Chemical Society, 1966; K. 23. Trozzolo, A. M. *Acc. Chem. Res.* **1968**, *1*, 329.

On the Equilibrium [10]Annulene⇌Bisnorcaradiene. X-ray Study of the β Form of 11-Methyltricyclo[4.4.1.$0^{1,6}$]undeca-2,4,7,9-tetraene-11-carbonitrile at Two Temperatures

Riccardo Bianchi, Tullio Pilati, and Massimo Simonetta*

Contribution from the Istituto di Chimica-Fisica e Centro C.N.R., Università, 20133 Milano, Italy.

Received February 3, 1981. Revised Manuscript Received June 9, 1981

Abstract: A new crystal phase (β form) of 11-methyltricyclo[4.4.1.$0^{1,6}$]undeca-2,4,7,9-tetraene-11-carbonitrile was studied by X-ray diffractometry at room temperature and at −100 °C. The unusually long C–C bond (mean value 1.817 Å), found in the previously studied phase (α form), is strongly reduced in the β form at room temperature (1.712 Å) and even more at −100 °C (1.622 Å). All other geometrical parameters vary in such a way as to emphasize the bisnorcaradiene character of the molecule. The remarkable dependence of the molecular geometry on crystal field and temperature suggests that the molecule is better described as a "fluxional system".

The geometry of a number of 1,6-methano[10]annulene derivatives has been determined in our laboratory in connection with the study of the equilibrium [10]annulene (**1**) ⇌ bisnorcaradiene (**2**).

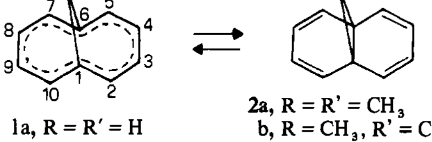

1a, R = R' = H
b, R = R' = F

2a, R = R' = CH$_3$
b, R = CH$_3$, R' = CN
c, R = R' = CN

It is known[1,2] that the introduction of π-donating groups at carbon C(1) in the cyclopropane ring lengthens all C–C bonds in the ring, while the introduction of π-acceptor substituents shortens the C(2)–C(3) bond and lengthens the other two. Hence, it can be argued that the 1,6 distance should decrease in the series **1b**, **1a**, **2a**, **2b**, **2c**. In fact Günther and Schmickler[3] showed that the ^{13}C NMR chemical shift of C(1) and C(6) changes system-

---

(1) R. Hoffman, *Proc. Int. Congr. Pure Appl. Chem.*, **23** (1971).

(2) R. Hoffman and R. B. Davidson, *J. Am. Chem. Soc.*, **93**, 5699 (1971).

(3) H. Günther and H. Schmickler, paper presented at the Second International Symposium on Non-benzenoid Aromatic Compounds, Lindau, Sept 23-27, 1974, ISNA II.

0002-7863/81/1503-6426$01.25/0

Table I. Crystal Data and Intensities Collection

$C_{13}H_{11}N$, Monoclinic, Space Group $C2/c$, $Z = 8$, $M_r = 181.24$

	room temp	−100 °C
	Crystal Data	
a, Å	21.316 (3)	21.304 (2)
b, Å	6.198 (1)	6.114 (1)
c, Å	15.660 (2)	15.535 (1)
β, deg	107.54 (1)	107.66 (1)
V, Å^3	1972.8	1928.1
d_{measd}, Mg/m^3, flotation	1.218	
d_{calcd}, Mg/m^3	1.220	1.249
cryst form	prism	sphere (by grinding)
dimens, mm	0.4 × 0.3 × 0.3	0.3 (diameter)
	Data Collection	
radiation	Mo Kα (λ = 0.71069 Å) graphite monocheomatized	
μ(Mo Kα), mm^{-1}	0.077	0.079
scan mode	$2\theta/\theta$	
scan width, deg	2.0 + $K\alpha_1 - K\alpha_2$ separation	
$(\sin\theta)/\lambda$ upper limit, Å^{-1}	0.650	0.857
scan rate, deg/min)	2.0–12.0	1.0–12.0
no. of check reflctns	3 (every 47 data)	6 (every 94 data)
no. of data collected	4684	11131
no. of independent data	2282	5108
no. of "observed data" (scan count > background)	2067	4688

atically and drastically in the above series. However, the X-ray analysis of crystal structures of **1a**,[4] **1b**,[5] **2a**,[6] and **2b**[7] showed an inversion in the C(1)–C(6) mean bond length for **2a** (1.799 Å) and **2b** (1.817 Å). These bonds are exceptionally long and furthermore vary over a wide range.[8] A qualitative explanation of these results was given[6,7] on the basis of the packing energy considerations and on the observation by Günther and Schmickler that for **2a** and **2b** the tautomers are very close in energy and are separated by a small energy barrier. It was also shown by ^{13}C NMR spectroscopy[3] that, when the temperature is decreased, the 1,6 distance lengthens in **2a** while it shortens in **2b**.

For the investigation of the dependence of geometrical parameters of **2b** on temperature and the study of the electron density along the C(1)–C(6) bond, a crystal structure determination at low temperature was undertaken. Good crystals of **2b**[9] were obtained by slow evaporation at 0 °C from a methanol solution. Surprisingly, these crystals were monoclinic.[8] Since observed and calculated densities are in good agreement, the existence of a new solid phase was postulated (β form). The new phase has been studied both at room temperature and at −100 °C. The study of the α form at low temperature was not undertaken, since this form is probably metastable below room temperature.[10]

Experimental Section and Structure Analysis

Cell parameters and intensity data were obtained at room temperature and at −100 °C on a computer-controlled diffractometer, Syntex P$\bar{1}$, equipped with the low-temperature LT-1 device (Syntex Analytical Instruments). The crystal used for low-temperature data collection was ground to a sphere both to eliminate anisotropic absorption effects and to reduce secondary extinction. Since our device does not have a permanent temperature control, the temperature was measured in absence of the crystal at the beginning and at the end of data collection. During data collection, the temperature stability was checked periodically by redetermining the values of cell parameters by using 15 standard reflections.

Table II. Results of Refinements

		−100 °C		
	room temp	LAD	AOD	HAD
no. of refined data	2066	2133	4688	2555
$(\sin\theta)/\lambda$ limits, Å^{-1}	0–0.650	0–0.650	0–0.857	0.650–0.857
R_W	0.047	0.044	0.050	0.048
R(with refined data)	0.071	0.039	0.059	0.084
R(with all data)	0.082	0.073	0.067	0.070[a]

[a] With overall scale factor.

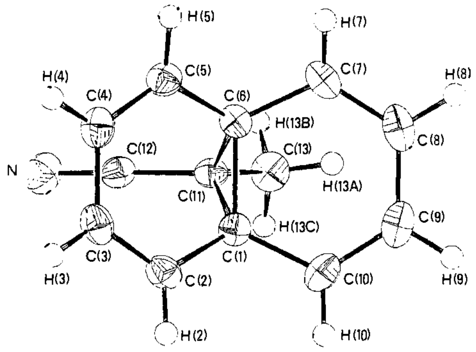

Figure 1. A view of **2b** at −100 °C along a principal axis of inertia with the numbering of atoms. Thermal ellipsoids for heavy atoms are drawn at a probability level of 50%; those of hydrogen atoms are not in scale.

The maximum variation of the cell volume was less than 1.0 Å^3 while the variation between room temperature and −100 °C was about 45.0 Å^3. The fluctuation of the temperature was estimated to be within ±2 °C.

Table I reports crystal data and details of data collection. The intensities were corrected for Lorentz and polarization effects but not for absorption. Their esd's were based on counting statistic plus a term $(0.03S)^2$, where S is the scan count, and the choice of the 0.03 value is due to the uncertainty in temperature control and fluctuations on check reflections intensities.

The structure was solved, using room-temperature data by a new program[11] based on rototranslation of a known rigid molecular model. Obviously, the model used was derived from the observed geometry of **2b** (α form).

The refinement was carried out by minimizing the function $\sum w(|F_o| - |F_c|)^2$, where $w = 4F_o/\sigma^2(F_o^2)$ for all observed reflections and $w = 0$ for all others. Scattering factors for C and N atoms were from Cromer and Waber[12] and those for hydrogen atoms from Stewart et al.[13] For the low-temperature structural analysis, besides the refinement with all observed data (AOD refinement), two more refinements were performed: one with low angle data ($(\sin\theta)/\lambda < 0.65$ Å^{-1}, LAD refinement) and the other one with high angle data ($(\sin\theta)/\lambda) > 0.65$ Å^{-1}, HAD refinement). In the HAD refinement, hydrogen parameters were fixed at the values derived from the AOD refinement. Due to the low ratio between scattering factors of H atoms and C and N atoms at $(\sin\theta)/\lambda > 0.65$ Å^{-1} and to the quality of our data, HAD refinement is not significant.[14,15] At the end of HAD refinement, the final value of the scale factor was determined from an AOD refinement with all other parameters fixed, to obtain more meaningful difference Fourier maps.[16] With use of these parameters, the function $\langle F_o/kF_c\rangle$ was analyzed according to Eisenstein.[17] As the function $\langle F_o/F_c\rangle$ was constant with respect to $(\sin\theta)/\lambda$,

---

(4) R. Bianchi, T. Pilati, and M. Simonetta, *Acta Crystallogr., Sect. B.*, **B36**, 3146 (1980).

(5) T. Pilati, and M. Simonetta, *Acta Crystallogr., Sect. B*, B32, 1912 (1976).

(6) R. Bianchi, G. Morosi, A. Mugnoli, and M. Simonetta, *Acta. Crystallogr., Sect. B*, **B29**, 1196 (1973).

(7) R. Bianchi, T. Pilati, and M. Simonetta, *Acta Crystallogr., Sect. B*, **B34**, 2157 (1978).

(8) The crystal structures of **2a** and **2b** (α form) are isomorphous, triclinic of space group $P1$ with two indipendent molecules in the unit cell. The individual values of the C(1)–C(6) bond lengths are 1.771 and 1.827 Å in **2a** and 1.783 and 1.851 Å in **2b**. Due to the strong dependence of these distances on crystal field, only molecules in similar environments should be compared.

(9) We are indebted to Professor E. Vogel for the gift of a sample of **2b**.

(10) The α form was obtained from a saturated solution in methanol near its boiling point.

(11) R. Bianchi, C. M. Gramaccioli, T. Pilati, and M. Simonetta, *Acta Crystallogr., Sect. A*, **A37**, 65 (1981).

(12) D. T. Cromer and J. T. Waber, *Acta Crystallogr.*, **18**, 104 (1965).

(13) R. F. Stewart, E. R. Davidson, and W. T. Simpson, *J. Chem. Phys.*, **42**, 3175 (1965).

(14) J. Almlöf and T. Ottersen, *Acta Crystallogr., Sect. A*, **A35**, 137 (1979).

(15) H. Hope and T. Ottersen, *Acta Crystallogr., Sect. B*, **B35**, 370 (1979).

(16) H. R. van der Wal, J. L. De Boer, and A. Vos, *Acta Crystallogr., Sect. A*, **A35**, 685 (1979).

(17) M. Eisenstein, *Acta Crystallogr., Sect. B* B35, 2614 (1979).

Table III. Hirshfeld Analysis of Thermal Motion[a]

	AOD parameters			HAD parameters		
bond	U_r	U_s	$\|\Delta U\|$	U_r	U_s	$\|\Delta U\|$
C(1)–C(2)	2509	2476	33	2356	2350	6
C(1)–C(6)	2881	2783	98	2707	2629	78
C(1)–C(10)	2616	2569	47	2512	2407	105
C(1)–C(11)	2008	2202	194	1875	2100	225
C(6)–C(5)	2529	2582	53	2408	2494	86
C(6)–C(7)	2523	2502	21	2381	2289	92
C(6)–C(11)	2156	2337	181	2081	2209	128
C(2)–C(3)	3948	3988	40	3635	3651	16
C(3)–C(4)	4359	4254	105	3937	3907	30
C(4)–C(5)	3572	3507	65	3133	3143	10
C(7)–C(8)	4380	4367	13	4047	4060	13
C(8)–C(9)	5688	5728	40	5297	5173	124
C(9)–C(10)	4472	4412	60	4015	4096	81
C(11)–C(13)	2291	2258	33	2188	2170	18
C(11)–C(12)	2731	3132	401	2727	2672	55
C(12)–N	3091	3141	50	2627	2694	67
root-mean-square of $\|\Delta U\|$			131			90

[a] For every couple of bonded atoms, the values $U_r = \mathbf{e}_k \mathbf{U}_r \mathbf{e}_k$ ($\times 10^5$ Å^2) are given (where $\mathbf{e}_k$ is the unit vector in the bond direction and $\mathbf{U}_r$ is the matrix of thermal parameters of the *r*th atom). ΔU is the difference between U_r and U_s.

Table IV. Atomic Coordinates and Equivalent or Isotropic Thermal Parameters[a]

Room Temperature

atom	x	y	z	B_{eq}
C(1)	0.34946 (7)	0.2029 (3)	0.32177 (9)	3.96 (6)
C(2)	0.28743 (8)	0.2889 (3)	0.32874 (12)	4.47 (7)
C(3)	0.25664 (8)	0.2079 (3)	0.38431 (12)	4.82 (8)
C(4)	0.27700 (9)	0.0147 (3)	0.43453 (12)	4.78 (8)
C(5)	0.32805 (9)	−0.1017 (3)	0.42902 (11)	4.45 (7)
C(6)	0.37318 (7)	−0.0300 (3)	0.38157 (10)	3.92 (6)
C(7)	0.40130 (8)	−0.1897 (3)	0.33543 (14)	4.92 (8)
C(8)	0.41322 (9)	−0.1524 (4)	0.25807 (15)	5.65 (10)
C(9)	0.39396 (9)	0.0437 (4)	0.20837 (13)	5.79 (10)
C(10)	0.36194 (9)	0.2036 (4)	0.23541 (11)	4.92 (8)
C(11)	0.40832 (7)	0.1859 (3)	0.40639 (10)	3.63 (6)
C(12)	0.39971 (7)	0.2910 (3)	0.48509 (11)	3.92 (6)
C(13)	0.47769 (9)	0.2171 (4)	0.40172 (15)	5.12 (8)
N	0.39644 (7)	0.3799 (3)	0.54715 (10)	5.48 (7)

atom	x	y	z	B_{iso}, Å^2
H(2)	0.2701 (8)	0.394 (3)	0.290 (1)	6.4 (5)
H(3)	0.2164 (9)	0.274 (3)	0.387 (1)	6.6 (4)
H(4)	0.2476 (8)	−0.039 (3)	0.470 (1)	7.0 (4)
H(5)	0.3343 (8)	−0.240 (3)	0.455 (1)	7.0 (5)
H(7)	0.4073 (11)	−0.323 (4)	0.363 (2)	9.0 (7)
H(8)	0.4321 (10)	−0.266 (3)	0.229 (1)	8.1 (5)
H(9)	0.4002 (8)	0.055 (3)	0.151 (1)	7.3 (4)
H(10)	0.3417 (9)	0.316 (3)	0.198 (1)	7.4 (5)
H(13A)	0.4856 (10)	0.146 (4)	0.349 (2)	10.0 (6)
H(13B)	0.5075 (11)	0.162 (4)	0.452 (2)	9.7 (6)
H(13C)	0.4886 (10)	0.363 (4)	0.394 (1)	10.4 (7)

−100 °C (HAD Parameters)

atom	x	y	z	B_{eq}
C(1)	0.34989 (4)	0.2003 (2)	0.32392 (5)	1.91 (2)
C(2)	0.28749 (4)	0.2963 (2)	0.32799 (6)	2.19 (2)
C(3)	0.25454 (4)	0.2152 (2)	0.38282 (7)	2.39 (2)
C(4)	0.27423 (5)	0.0156 (2)	0.43361 (7)	2.37 (3)
C(5)	0.32654 (5)	−0.1031 (2)	0.42953 (7)	2.16 (3)
C(6)	0.37162 (4)	−0.0246 (1)	0.38061 (6)	1.90 (2)
C(7)	0.40088 (5)	−0.1932 (2)	0.33716 (8)	2.44 (3)
C(8)	0.41400 (6)	−0.1567 (3)	0.25833 (10)	2.88 (4)
C(9)	0.39528 (6)	0.0457 (3)	0.20786 (8)	2.87 (3)
C(10)	0.36325 (5)	0.2098 (2)	0.23628 (6)	2.49 (3)
C(11)	0.40884 (4)	0.1907 (1)	0.40996 (5)	1.80 (2)
C(12)	0.39900 (4)	0.2952 (2)	0.48818 (5)	2.49 (3)
C(13)	0.47861 (4)	0.2211 (2)	0.40631 (8)	1.96 (2)
N	0.39409 (6)	0.3862 (2)	0.55126 (7)	2.69 (3)

atom	x	y	z	B_{iso}, Å^2
H(2)	0.2719 (6)	0.414 (2)	0.2910 (8)	3.9 (2)
H(3)	0.2154 (6)	0.283 (2)	0.3834 (7)	3.4 (2)
H(4)	0.2453 (5)	−0.041 (2)	0.4648 (8)	3.9 (2)
H(5)	0.3336 (6)	−0.248 (2)	0.4530 (8)	3.8 (2)
H(7)	0.4081 (6)	−0.326 (2)	0.3640 (8)	4.5 (3)
H(8)	0.4316 (6)	−0.281 (2)	0.2325 (9)	4.9 (3)
H(9)	0.4011 (6)	0.063 (2)	0.1505 (9)	5.2 (3)
H(10)	0.3454 (6)	0.328 (2)	0.1983 (9)	4.6 (3)
H(12A)	0.4884 (8)	0.136 (3)	0.3595 (11)	7.4 (4)
H(12B)	0.5097 (7)	0.167 (2)	0.4592 (10)	5.7 (3)
H(12C)	0.4874 (7)	0.373 (3)	0.3973 (10)	6.3 (4)

[a] B_{eq} has been calculated by $B_{eq} = 8\pi^2 U_{eq}$, where U_{eq}, where $U_{eq} = {}^1/_3(U_{11} + U_{22} + U_{33})$.

no correction was considered to be necessary. The secondary extinction parameter was set equal to zero because the refined value was less than its esd. Results from various refinements are collected in Table II.

The LAD refinement was carried out in order to compare the geometry of the molecule at room and at low temperature. Hereafter, we will refer to the geometrical parameters derived from LAD refinement for comparison among **2b** (α and β forms), **1a**, and **1b**.

All the maps, reported in the figures, are calculated with the HAD parameters. The HAD refinement gives more realistic geometrical and thermal parameters because it reduces the bias due to the free atom model. Fourier difference maps, calculated with AOD and LAD parameters, show some nonrealistic features: for example, in the middle of the C–N bond there is a trough. On the contrary, the corresponding map, derived from the HAD parameters, shows a peak along the C–N bond. Moreover, the Hirshfeld motion analysis[18] indicates that the AOD thermal parameters are less correctly determined than the HAD ones. The "rigid-bond" postulate asserts that the relative vibrational motion of a pair of bonded atoms has an effectively vanishing component in the direction of the bond. It follows that for every pair of atoms connected by a covalent bond the mean square amplitudes along the bond are equal. If the vibration parameters from a given refinement satisfy this equality, within the expected tolerance (0.001 Å^2 for heavy atoms such as carbon and nitrogen), we have good, objective evidence of the physical acceptability of the results. The analysis of the deviations can be used to check the goodness of a set of thermal parameters. Table III reports the results of Hirshfeld analysis for AOD and HAD thermal parameters. It can be deduced that the vibration parameters, derived from the HAD refinement, are more acceptable.

Table IV reports the final atomic coordinates together with equivalent or isotropic thermal parameters at room and at low temperature.

Figure 1 shows a projection of the molecule at −100 °C together with the numbering scheme. Thermal ellipsoids are drawn at 50% probability level.

Geometry of 2b and Relations with Omologue Compounds

Tables V and VI list bond distances and angles, obtained from room-temperature structural analysis and from low-temperature HAD and LAD refinements.

The most interesting feature of **2b** is the strong dependence of its geometrical parameters on crystal field and temperature. The largest effect is the variation of the C(1)–C(6) bond length from 1.851 Å in **2b** (α form, molecule A) to 1.640 Å (or 1.622 Å with the HAD parameters) in **2b** (β form) at −100 °C. This remarkable change of the 1,6 distance involves also a less evident but systematic variation of all the geometrical parameters of **2b**. A function of these parameters which has chemical meaning, is $\rho = \langle (r_j - \bar{r})^2 \rangle^{1/2}$, where the r_j's are the bond distances along the annulenic perimeter and $\bar{r}$ is their average. According to Gavezzotti and Simonetta's work,[19] ρ decreases as the aromatic character of the molecule increases. In **2b** lengthening of the 1,6 distance is followed by the systematic decreasing of ρ.

Table VII shows the correlation between ρ and the 1,6 distance in **2a**, **1a**, and **1b** and in the four experimental geometries of **2b**. The lengthening of the 1,6 distance and the corresponding shortening of C(1)–C(11) and C(6)–C(11) bonds involves the reduction of the distance of C(11) from the middle point of the

---

(18) F. L. Hirshfeld, *Acta Crystallogr., Sect. A*, **A32**, 239 (1976).

(19) A. Gavezzotti and M. Simonetta, *Helv. Chim. Acta*, **59**, 2984 (1976).

Table V. Bond Lengths (Å)[a]

	room temp		−100 °C (HAD set)		−100 °C (LAD set)	
bond	length	mean	length	mean	length	mean
C(1)–C(6)	1.712		1.622		1.640	
C(1)–C(11)	1.529	1.527	1.533	1.533	1.535	1.534
C(6)–C(11)	1.525		1.533		1.533	
C(1)–C(2)	1.460	1.456	1.472	1.473	1.474	1.472
C(5)–C(6)	1.451		1.474		1.470	
C(1)–C(10)	1.455	1.456	1.474	1.472	1.472	1.471
C(6)–C(7)	1.457		1.470		1.469	
C(2)–C(3)	1.336	1.333	1.352	1.350	1.340	1.341
C(4)–C(5)	1.330		1.347		1.341	
C(7)–C(8)	1.331	1.337	1.355	1.358	1.345	1.344
C(9)–C(10)	1.342		1.360		1.342	
C(3)–C(4)	1.427		1.445		1.443	
C(8)–C(9)	1.434		1.454		1.445	
C(11)–C(12)	1.454		1.443		1.450	
C(11)–C(13)	1.515		1.516		1.517	
C(12)–N	1.138		1.159		1.147	
C_{sp^2}–H	0.89–1.01		0.90–0.98		0.92–1.00	
C(13)–H	0.92–0.99		0.94–0.97		0.94–0.97	
σ(C–C, C–N)	0.002–0.003		0.001–0.002		0.001–0.002	
σ(C–H)	0.014–0.027		0.009–0.018		0.010–0.016	

[a] Standard deviations and C–H bonds are given in range only. The values are grouped assuming *m* symmetry, and mean values are also given.

Table VI. Bond Angles (Deg)[a]

	room temp		−100 °C (HAD set)		−100 °C (LAD set)	
	angle	mean	angle	mean	angle	mean
C(1)–C(11)–C(6)	68.2		63.91		64.60	
C(1)–C(6)–C(11)	56.0	55.9	58.05	58.04	57.74	57.70
C(6)–C(1)–C(11)	55.8		58.04		57.65	
C(2)–C(1)–C(6)	113.1	113.6	115.29	115.46	114.71	114.99
C(5)–C(6)–C(1)	114.0		115.62		115.27	
C(10)–C(1)–C(6)	113.9	113.7	115.56	115.70	115.14	115.01
C(7)–C(6)–C(1)	113.5		115.83		114.88	
C(2)–C(1)–C(10)	119.5	119.2	116.99	116.60	117.81	117.57
C(5)–C(6)–C(7)	118.8		116.21		117.32	
C(2)–C(1)–C(11)	119.0	119.2	119.31	119.18	119.07	119.00
C(5)–C(6)–C(11)	119.3		119.03		118.93	
C(10)–C(1)–C(11)	118.3	118.5	118.05	118.54	118.01	118.30
C(7)–C(6)–C(11)	118.6		119.03		118.59	
C(1)–C(2)–C(3)	123.1	123.2	121.95	121.87	122.27	122.18
C(4)–C(5)–C(6)	123.3		121.78		122.09	
C(6)–C(7)–C(8)	123.6	123.3	122.14	121.98	122.75	122.47
C(1)–C(10)–C(9)	122.9		121.81		122.19	
C(2)–C(3)–C(4)	123.2	122.9	122.26	122.35	122.54	122.51
C(3)–C(4)–C(5)	122.6		122.43		122.47	
C(7)–C(8)–C(9)	122.6	122.8	121.96	122.16	121.94	122.37
C(8)–C(9)–C(10)	123.0		122.35		122.79	
C(1)–C(11)–C(13)	120.5	120.7	121.07	121.16	120.80	120.95
C(6)–C(11)–C(13)	120.8		121.25		121.10	
C(1)–C(11)–C(12)	115.1	115.3	115.30	115.59	115.38	115.61
C(6)–C(11)–C(12)	115.5		115.87		115.83	
C(12)–C(11)–C(13)	111.0		111.82		111.77	
C(11)–C(12)–N	175.8		176.24		176.18	
C_{sp^2}–C_{sp^2}–H	116.1–123.1		116.6–121.6		116.0–121.9	
C_{sp^3}–C_{sp^2}–H	113.0–118.2		116.5–117.2		115.7–116.2	
C(11)–C(13)–H	110.2–114.0		111.0–113.6		110.9–113.7	
H–C–H	101.9–109.3		102.2–110.3		102.5–110.0	
σ(C–C–C,C–C–N)	0.1–0.2		0.05–0.13		0.06–0.10	
σ(C–C–H)	0.8–1.6		0.6–0.8		0.5–0.8	
σ(H–C–H)	1.7–2.0		1.1–1.3		1.1–1.2	

[a] Values involving hydrogen atoms and esd's are given in range only. The values are grouped assuming *m* symmetry, and mean values are also given.

1,6 distance (*h* in Table VIII). This means that the interaction between the annulene perimeter and the groups bonded at C(11) increases and it induces systematic variations of the geometrical parameters involved in the interaction. Some of these parameters are summarized in the Table VIII.

These drastic and systematic variations in the molecular parameters of **2b** are consistent for the four experimental geometries and they pose the problem of their chemical meaning. The experimental results can be considered as four snapshots at different stages of advancement of the reaction [10]annulene ⇄ bisnorcaradiene. The low-temperature result shows clearly that the ground state of **2b** is bisnorcaradienic. On the other hand, from the three different molecular geometries of **2b** at room temperature one can suppose that the molecular energy has another minimum corresponding to the [10]annulene tautomer with a very low energetic difference with respect to the ground state and with a

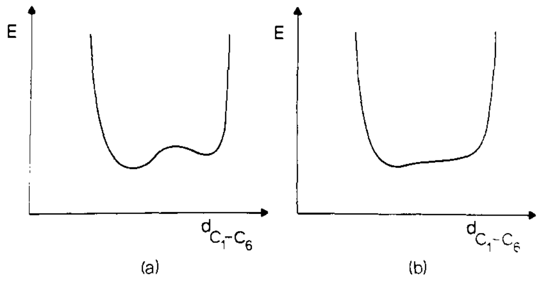

Figure 2. Potential energy profiles.

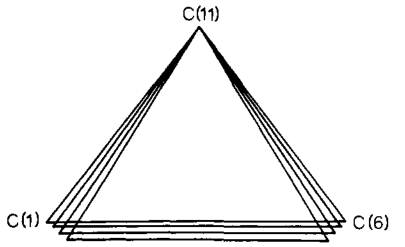

Figure 3. Superposition of the four experimental cyclopropane rings of **2b**, drawn with C(11) as common origin and with the assumption of *m* symmetry.

Table VII. Correlation between $\rho = \langle (r_j - \bar{r})^2 \rangle^{1/2}$ and 1,6 Distance in Some Bisnorcaradiene and [10]Annulene Derivatives

molecule	1,6 distance, Å	ρ, Å
2b, β form at −100 °C	1.640	0.060
2b, β form at room temp	1.712	0.056
2a, molecule B	1.771	0.056
2b, α form, molecule B	1.783	0.052
2a, molecule A	1.827	0.049
2b, α form molecule A	1.851	0.041
1a	2.235	0.017
1b	2.269	0.023

low-energy barrier between the two states (Figure 2a). Another possibility is that the bisnorcaradienic tautomer has an asymmetric potential energy function with a very flat minimum (Figure 2b). In the last hypothesis the vibrational levels would be very close. With both model one can assign the experimental parameters to a weighted average of the two minimum energy geometries (first hypothesis) or of the various geometries of the occupied vibrational levels (second hypothesis). We rationalize the existence of three different geometries at room temperature as a consequence of the influence of three different crystal fields on the free molecule potential. At this point a conclusion can be inferred: although the ground-state conformation of **2b** is bisnorcaradienic, the molecule is better described as a "fluxional system" according to the definition of Günther and Schmickler.[3]

Since **2b** (α form) is probably metastable at room temperature,[10] the best comparison between **2a** and **2b** is made with the β form.[20]

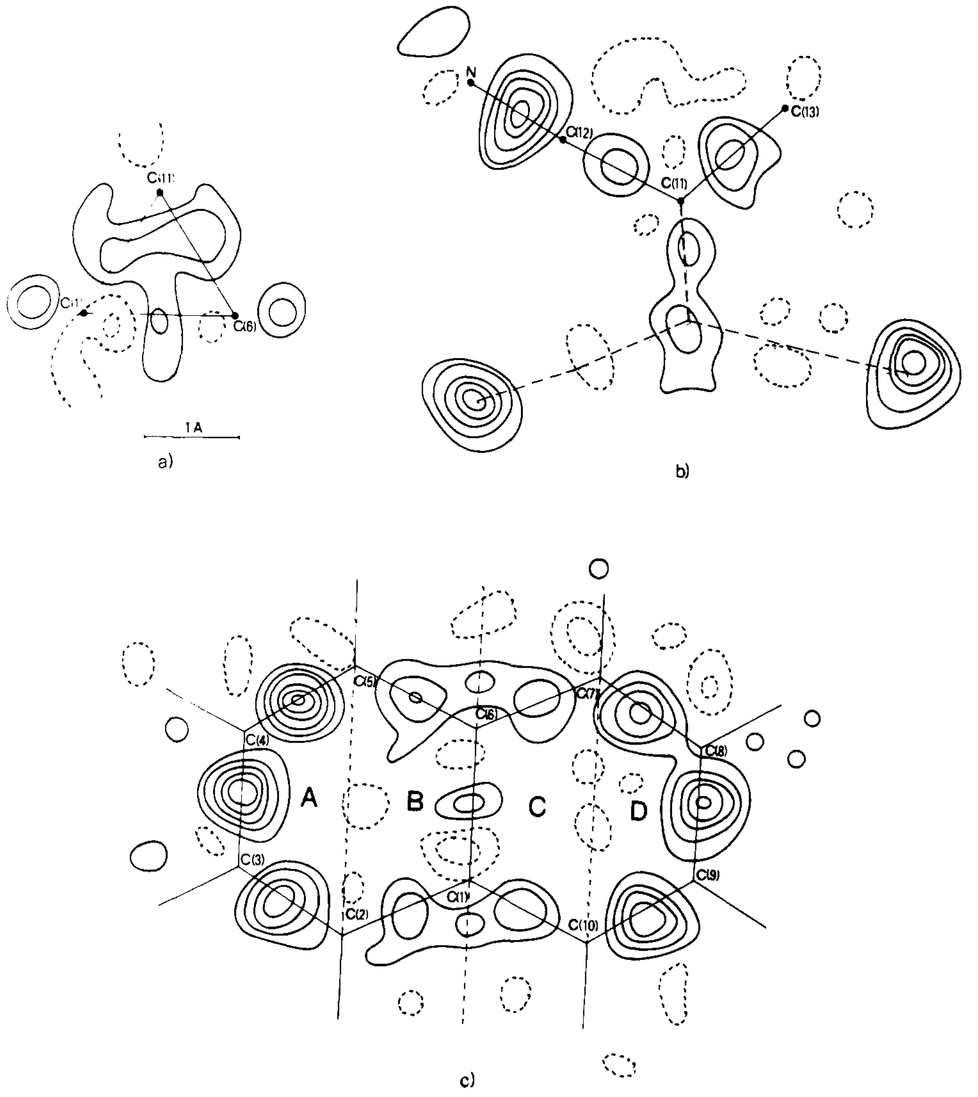

Figure 4. Relevant Fourier difference maps (contours levels are at interval of 0.1 e Å^{-3}, solid lines positive, dashed lines negative, and zero contours omitted): (a) plane of the cyclopropane ring; (b) plane containing C(11), C(12), C(13), and N atoms; bonds above and below the plane are represented with different lines; (c) composition of the four maps for the molecular planes *A*, *B*, *C*, and *D* defined in Table VIII.

Table VIII. Systematic Variation of Geometrical Parameters of **2b** vs. the Distance (*h*) between C(11) and the Middle Point of the C(1)–C(6) bond[a]

	β form		α form		
parameter	−100 °C	room temp	mol B	mol A	Δ-(max)
h^b	1.297	1.265	1.220	1.192	0.105
C(1)–C(11)[b]	1.535	1.529	1.508	1.508	0.027
C(6)–C(11)[b]	1.533	1.525	1.514	1.511	0.022
C(12)–C(11)–C(13)[c]	111.8	111.0	108.7	107.6	4.2
C(11)–C(12)–N[c]	176.2	175.8	175.3	174.7	1.5
C(1)–C(2)–C(3)–C(4)[c]	6.8	7.6	9.8	12.9	6.1
C(3)–C(4)–C(5)–C(6)[c]	6.9	8.7	10.6	12.0	5.1
C(6)–C(7)–C(8)–C(9)[c]	4.8	5.8	7.7	8.5	3.7
C(8)–C(9)–C(10)–C(1)[c]	4.7	6.3	7.5	9.7	5.0
$A\wedge B^c$	173.6	172.6	170.7	168.8	4.8
$B\wedge C^c$	141.3	140.4	139.6	138.5	2.8
$C\wedge D^c$	175.6	174.5	173.1	171.8	3.8

[a] The least-squares planes are through C(2), C(3), C(4), C(5) (*A*), C(1), C(2), C(5), C(6) (*B*), C(1), C(6), C(7), C(10) (*C*), and C(7), C(8), C(9), C(10) (*D*). Torsional angles are given with their absolute values. In the last column the difference between maximum and minimum values of each parameter is reported. [b] In angstroms. [c] In degrees.

The theoretical prediction that the 1,6 distance in **2b** must be shorter in **2a** is now confirmed by the experiment. On the other hand, this prediction is true even if the comparison is made between averaged values: namely, 1.799 Å for **2a** and 1.782 Å for **2b**.

Correlation between Refined Parameters and Fourier Difference Residuals

2b is not a rigid molecule. This is true at room temperature, but even at −100 °C, because the internal modes are not negligible, in particular for the vibrational modes involving C(1) and C(6) atoms. We divide the values of Table III (HAD parameters) in two classes: one containing the values involving the atoms C(1) and C(6) and the other involving the remaining atoms. The root-mean-square of $|\Delta U|$ for both classes are 0.001 20 and 0.000 59 Å^2, respectively. This indicates that the bonds of the first class are less rigid than the second ones. With the assumption that the experimental geometries are four snapshots of the molecular motion, it can be easily seen (Figure 3) that the most important internal contribution to the motion of C(1) and C(6) is the bending of the C(1)–C(11)–C(6) angle.

The motion of C(1) and C(6) atoms due to this bending is not linear, and moreover it is anharmonic because of the weakness of the C(1)–C(6) bond. Hence, a correct analysis of X-ray data would also include third and fourth cumulant terms in the expression for calculated structure factor. Unfortunately, for this analysis the observed data/parameters ratio becomes too low and the quality of our data is not good enough. A significant estimation of the structural parameters from such a refinement is not possible. No attempts in this direction were made, and hence the HAD parameters are not completely satisfactory especially for C(1) and C(6). In fact, difference maps in the plane of the cyclopropane ring (Figure 4a) and in the plane perpendicular to this, through C(11) and the middle point of the 1,6 bond (Figure 4b), have unusual features. In these difference maps only a slim evidence for the three expected positive residues[21] outside the ring appears. The troughs and peaks along the C(1)–C(6) direction and the residues around C(11) could indicate a departure from the normal distribution of the istantaneous position of the cyclopropane ring atoms. On the contrary, the maps for other planes reported in Figure 4c (planes A and D) and in Figure 5 are more significant from the chemical point of view. The absence of cylindrical symmetry of the residues along C(12)–N (Figure 5a) and C-(3)–C(4) (Figure 4c) bonds is probably due to their closeness and mutual polarization.

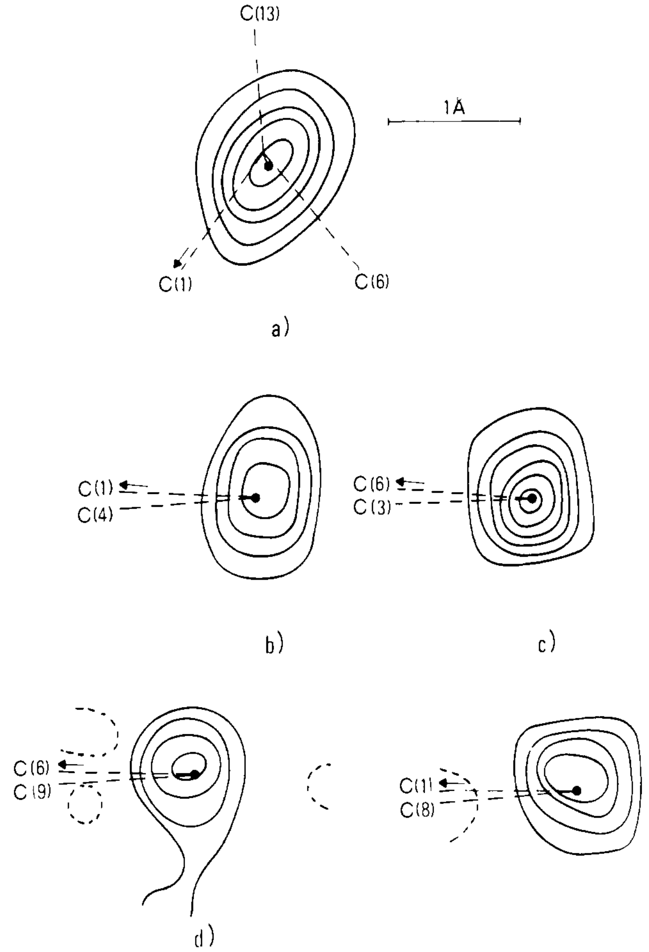

Figure 5. Section perpendicular to some bonds through the middle point (contours are as in Figure 4): (a) for C(12)–N triple bond; (b–e) for C(2)–C(3), C(4)–C(5), C(7)–C(8), and C(9)–C(10) double bonds, respectively.

In conclusion, from the low-temperature X-ray investigation we have produced evidence of the existence of the C(1)–C(6) bond. This finding could be reinforced by a more adequate treatment of the thermal motion.

Acknowledgment. We thank Professor E. Vogel for kindly providing us with a sample of the title compound.

Supplementary Material Available: Listings of observed and calculated structure factor amplitudes (at room temperature, Table SI, and at −100 °C, Table SII) and tables of anisotropic thermal parameters (at room temperature, Table SIII, and at −100 °C, Table SIV) (31 pages). Ordering information is given on any current masthead page.

---

(20) All our attempts to obtain another phase of **2a** failed. Günther and Schmickler found that the chemical shift of C(1) and C(6) in **2a** has an opposite temperature dependence with respect to **2b**. For this reason we think that for **2a** the existence of a phase comparable with β form of **2b** is very unlikely.

(21) A. Hartman and F. L. Hirshfeld, *Acta Crystallogr.*, **20**, 80 (1966).